Received: 6 March 2021 | Accepted: 19 April 2021

DOI: 10.1111/1759-7714.13990

ORIGINAL ARTICLE

WILEY

Clinical-radiological characteristics and intestinal microbiota in patients with pancreatic immune-related adverse events

Bei Tan[1] | Min-jiang Chen[2] | Qi Guo[3] | Hao Tang[4] | Yue Li[1] | Xin-miao Jia[5] | Yan Xu[2] | Liang Zhu[6] | Meng-zhao Wang[2] | Jia-ming Qian[1]

[1]Department of Gastroenterology, Peking Union Medical College Hospital, Chinese Academy of Medical Science & Peking Union Medical College, Beijing, China

[2]Department of Respiratory and Critical Care Medicine, Peking Union Medical College Hospital, Chinese Academy of Medical Science & Peking Union Medical College, Beijing, China

[3]Department of Gynecology & Obstetrics, Peking Union Medical College Hospital, Chinese Academy of Medical Science & Peking Union Medical College, Beijing, China

[4]Department of Internal Medicine, Peking Union Medical College Hospital, Chinese Academy of Medical Science & Peking Union Medical College, Beijing, China

[5]Medical Research Center, Peking Union Medical College Hospital, Chinese Academy of Medical Science & Peking Union Medical College, Beijing, China

[6]Department of Radiology, Chinese Academy of Medical Science & Peking Union Medical College, Beijing, China

Correspondence

Yan Xu, Department of Respiratory and Critical Care Medicine, Peking Union Medical College Hospital, Chinese Academy of Medical Science & Peking Union Medical College, Beijing China, No.1 Shuaifuyuan, Dongcheng District, Beijing 100730, China.
Email: maraxu@163.com

Liang Zhu, Department of Radiology, Peking Union Medical College Hospital, Chinese Academy of Medical Science & Peking Union Medical College, Beijing China, No.1 Shuaifuyuan, Dongcheng District, Beijing 100730, China.
Email: dancingfox1217@163.com

Funding information

Natural Science Foundation of Beijing Municipality, Grant/Award Number: 7192172; National Natural Science Foundation of China, Grant/Award Numbers: 82000526, 82003309

Abstract

Background: The pancreatic immune-related adverse event (irAE) is a rare but increasingly occurrence disease with limited knowledge, which was associated with the use of immune checkpoint inhibitors (ICIs).

Methods: In this case series study of pancreatic irAE patients, clinical and radiological manifestations are summarized. Baseline and post-treatment fecal microbiota of immune-related acute pancreatitis (irAP) patients were analyzed by the 16 s rDNA amplicon sequencing method.

Results: A total of six patients were enrolled into the study, and the onset of pancreatic irAEs occurred a median of 105 days after a median of 4.5 cycles with immune checkpoint inhibitors (ICIs). All patients had an effective response to ICIs. Abdominal pain was the main clinical manifestation. Serum amylase (sAMY) and lipase (sLIP) had dynamic changes parallel to clinical severity. Contrast-enhanced computed tomography (CT) did not accurately reveal the level of inflammation. However, magnetic resonance imaging (MRI) was a sensitive imaging method which showed decreased and increased signal intensity of pancreatic parenchyma in T1-weighted fat-saturated and diffusion-weighted imaging, respectively. Glucocorticoids were the main treatment with a rapid initial effect followed by a slow improvement. After reinitiation of ICI therapy, pancreatic irAEs either deteriorated, remained stable or the patient developed severe pancreatic β-cell destruction without irAP recurrence. The baseline microbiota of irAP had low Bacteroidetes/Firmicutes ratio at phylum level, low relative abundance of Alistipes, Bacteroides and high Lachnospiraceae at genus level, compared to levels of pancreatic β-cell destruction and post-treatment of irAP.

Conclusions: Pancreatic irAE patients had corresponding abdominal pain and increase in sAMY/sLIP. MRI was found to be an ideal imaging modality. Treatment with glucocorticoids were the main approach. The microbiota showed relative changes at baseline and during treatment.

KEYWORDS

immune checkpoint inhibitors, immune-related adverse events, microbiota, pancreatic disease

INTRODUCTION

Immunotherapy is revolutionizing the treatment paradigm for a broad spectrum of malignancies. Immune checkpoint inhibitors (ICIs) include antiprogrammed cell death protein 1 (PD-1)/programmed cell death ligand 1 (PD-L1) and anti-cytotoxic T lymphocyte-associated antigen-4 (CTLA-4). However, coupled with these landmark successes in cancer treatment are a series of immune-related adverse events (irAEs). These are a series of unique challenges caused by T cell activation which can affect many organs. When irAEs occur, ICI therapy may be interrupted or permanently discontinued, leading to tumor progression in patients and decreased survival. Thus, they remain a major bottleneck of tumor immunotherapy.

With the expansion in use of ICIs, oncologists have gradually become familiar with the common digestive system irAEs (e.g., immune-related colitis or hepatic toxicity). Pancreatic irAEs are rare but are increasing in occurrence, and include asymptomatic serum amylase (sAMY) or serum lipase (sLIP) elevations (Asy-sAMY/sLIP-Elv) and symptomatic immune-related acute pancreatitis (irAP). A systematic review and meta-analysis identified the incidence of asymptomatic sLIP elevation and grade 2 pancreatitis after ICIs to be 2.7% (211/7702) and 1.9%(150/7702), respectively.[1] Of patients with irAEs attending the emergency department, 0.9%–1.9% had acute pancreatitis (AP).[2] The pancreatic irAEs present as typical symptoms, CT findings and long-term adverse outcomes similar to those of acute pancreatitis.[3] However, our knowledge of pancreatic irAEs remains limited.

With the consecutive publication of three high-profile articles, the role of intestinal microbiota in immunotherapy has attracted increasing attention. Several studies have revealed that patient microbiota affected the efficacy of ICIs in different tumors.[4–6] Further studies showed that ICI-related colitis did not occur in germ-free mice, thus the occurrence depends on the presence of intestinal microbiota.[7] The baseline intestinal microbiota predicts both the clinical response and colitis in ICI-treated patients.[8] Fecal microbiota transplantation (FMT) has been previously reported to effectively treat ICI-related colitis refractory to glucocorticoid and biological therapy, and supplementation of probiotics has been shown to effectively reduce ICI-related colitis in mice.[9–11] Studies have also shown that the microbiota of autoimmune pancreatitis (AIP) is different in patients with chronic pancreatitis (CP).[12] However, the role of intestinal microbiota in pancreatic irAEs has not been previously explored.

Thus, in this study, we aimed to describe the characteristics of pancreatic irAEs, including clinical and radiological manifestations, ideal biomarkers, treatment and outcomes, and reinitiation of ICIs, as well as to explore the potential role of microbiota in driving pancreatic irAEs. The aim of the study was to provide new insights into the prevention and management of pancreatic irAEs.

METHODS

Patients

The detailed history of all patients with malignant tumors who received ICI therapy from January 2018 to December 2020 were collected. Patients who met the following criteria and had been diagnosed with pancreatic irAEs were included in our study: (i) Patients with advanced malignant tumors confirmed by pathology, (ii) treatment with ICIs including anti-PD-1 and/or anti-CTLA-4, (iii) patients diagnosed with Asy-sAMY/sLIP-Elv or acute pancreatitis according to NCCN guidelines on ICI-related toxicities[13] and (iv) other causes of pancreatic injury were excluded, including, but not limited to, cholelithiasis, hyperlipidemia, alcohol, abnormal anatomy and chemotherapy drugs.

This study was approved by the Ethical Committee of Peking Union Medical College Hospital (No. S-K1557). Informed consent was obtained from all patients for use of their clinical data, imaging materials, and the collection of fresh feces for microbiota analysis.

Demographic and clinical data source

Demographic and clinical data including gender, age, clinical stage, surgery, chemotherapy and immunotherapy, duration from ICIs to irAEs, symptoms, laboratory results, irAE treatment, outcomes and reinitiation of ICIs were all retrieved from the electronic medical records system.

Radiological studies

Computed tomography (CT) examination was performed using a 128-row multidetector CT scanner (Somatom Definition Flash). The scanning parameters were tube voltage 120 kVp, effective amperage settings 150 mAs, and slice thickness 3 mm. After an unenhanced scan of the upper abdomen, dynamic contrast-enhanced scans were acquired at 15 s after aortic enhancement of 100 HU (pancreatic phase), and 30 s and 90 s later (portal venous phase and delayed phase), respectively.

Magnetic resonance cholangiopancreatography (MRCP) and contrast-enhanced magnetic resonance imaging (MRI) were performed on a 3 T MR scanner (MAGNETOM Skyra, Siemens). The sequences included volume-interpolated breath-hold (VIBE) T1-weighted imaging, and turbo spin echo (TSE) fat saturated (fs) T2W1. Half-Fourier acquisition single-shot turbo spin echo (HASTE) T2WI in coronal and axial plane (TR/TE 2000/92 ms, FOV, 300 × 300, slice thickness 4 mm), and diffusion-weighted image (DWI) with b values of 0 and 800 mm^2/s. 3D MRCP and thick-slab 2D MRCP were both performed. A multiphase contrast-enhanced study was performed after patients had been injected with gadobenate dimeglumine intravenously.

Peripheral blood T lymphocyte subsets analysis

The analysis of T lymphocyte subsets was routinely tested in the clinical laboratory. Peripheral blood with ethylenediamine tetra-acetic acid (EDTA) anticoagulation was measured by polychromatic flow cytometer (EPICS2XL, Beckman-Coulter). The T lymphocyte subsets were counted, including the percentage of $CD4^+$ in T cell, $CD8^+$ in T cell, as well as two main activation subsets HLA-DR^+CD8^+ in $CD8^+$ T cell, and $CD38^+CD8^+$ in $CD8^+$ T cell.

Intestinal microbiota analysis

Fresh feces were collected at different timepoints of three irAP patients as follows. Pt.1A: onset of irAP in a patient with severe irAP; Pt.1B: two weeks after glucocorticoid treatment in a patient with severe irAP; Pt.1C: four weeks after glucocorticoid treatment in a patient with severe irAP; Pt. 1D: six weeks after glucocorticoid treatment in a patient with severe irAP; Pt. 1E: 13 weeks after glucocorticoid treatment in a patient with severe irAP. Pt. 2A: onset of pancreatic β-cell destruction with irAP recovery in a patient with moderate irAP. Pt. 3A: onset of irAP in a patient with mild irAP.

The microbiota was analyzed by 16 s rDNA amplicon sequencing method on an Illumina MiSeq (PE300) sequencing platform. Operational taxonomic units (OTUs) were detected by QIIME2, and used to draw the relative ternary diagram, flower plot and principal coordinates analysis (PCoA). The α diversity was assessed by observed species, Shannon, Simpson, Chao1, ACE indexes and rank abundance curve. The differences of microbiota composition were compared by relative abundance at phylum and genus levels, and the relative histogram and line chart were drawn.

RESULTS

Demographic and clinical characteristics

A total of six patients were enrolled into our case series study including patients with severe, moderate, mild irAPs and three Asy-sAMY/sLIP-Elv patients. There were six patients (four males and two females) with a median age of 66 (range 38–71) years. They all had advanced carcinoma which included three non-small cell lung cancers (NSCLCs), two small cell lung cancers (SCLCs), and one uterine endometrial dedifferentiated cancer. Pancreatic immune-related adverse events occurred a median of 105 (range 10–171) days from the first ICI treatment, and 5.5 (range 1–18) days from the last ICI treatment. The median cycle was 4.5 (range 1–7) with anti-PD-1 monotherapy or combined therapy. Immunotherapy of all patients was effective, with a complete response (CR) in one patient, two partial responses (PRs) and three patients with stable disease (SD).

Abdominal pain was the main clinical manifestation, which was absent to severe in Asy-sAMY/sLIP-Elv to severe irAP patients. The patients with severe, moderate and mild irAP had corresponding severe (visual analogue scale 7–8 of 10), mild (visual analogue scale 2–3 of 10) and nausea without abdominal pain. Pancreatic irAEs could be accompanied by other irAEs. The patients with moderate and mild irAP developed mild (grade 1) and severe (grade 3) dermatological AEs. One Asy-sAMY/sLIP-Elv occurred with severe recurrent colitis (grade 3) and mild transaminitis without elevated bilirubin (grade 1) (Table S1).

Laboratory results

Serum amylase and lipase

In patients with irAP, sAMY and sLIP had dynamic changes parallel with clinical conditions. These are ideal indicators for assessment and monitoring of irAP severity. At the onset of irAP, sAMY and sLIP increased to 1263 U/L (normal range 25–115 U/L) and 14 970 U/L (normal range 73–393 U/L) in the patient with severe irAP. These were 158 U/L and 1179 U/L in the patient with moderate irAP, 192 U/L and 3135 U/L in the patient with mild irAP (Figure S1A, S1B and S1C). In the patient with severe irAP, the sAMY and sLIP decreased to 686 U/L and 10 517 U/L after traditional treatment, 498 U/L and 5002 U/L after two weeks of prednisone, 215 U/L and 1219 U/L after eight weeks of prednisone. Finally, after 22 weeks treatment of prednisone, the sAMY and sLIP decreased to normal with 112 U/L and 285 U/L, respectively (Figure S1A, Table S2). In the patients with moderate and mild irAP, the sAMY and sLIP returned to normal within two days after traditional treatment and methylprednisolone (Figures S1B and S1C, Tables S3 and S4).

In the patients with Asy-sAMY/sLIP-Elv, the sAMY and sLIP were also parallel to clinical conditions. The sAMY/sLIP significantly increased in patients with continued anti-PD-1 treatment with deterioration to moderate irAP in the first Asy-sAMY/sLIP-Elv patient. The sAMY/sLIP significantly decreased after glucocorticoid treatment for moderate irAP in the first patient, fasting and fluid hydration therapy in the second patient, and glucocorticoid treatment for coexisting severe colitis in the third patient (Figures S1D–F, Table S5).

Serum IgG4 level

Serum IgG4 was mildly elevated in the patient with severe irAP, did not fulfill the criterion of IgG4-related disease three-fold increase. In the patient with severe irAP, there was a 1.9-fold increase of 2430 mg/L (80–1300 mg/L) in the serum IgG4 which returned to normal after three weeks of glucocorticoid treatment (Table S2). In patients with mild

and moderate irAP, serum IgG4 was within normal limits (590 mg/L and 219 mg/L, respectively).

T lymphocyte subsets

Peripheral blood T lymphocyte subsets did not ideally reflect the activation and changes of T cell immunity in pancreatic irAE patients. Only the percentage of HLA-DR^+CD8^+ in $CD8^+$ T cells increased at the onset of pancreatic irAEs in all patients, but were not parallel with the severity. The severe, moderate and mild irAP patients had 250%, 42.4% and 28.2% increase respectively, as well as a 36.1%–110% increase in three Asy-sAMY/sLIP-Elv patients. Furthermore, other markers including the percentage of $CD4^+$ in T cell, $CD8^+$ in T cell, and $CD38^+CD8^+$ in $CD8^+$ T cell had inconsistent changes in all patients (Figure S2, Table S2 and S6).

Radiological characteristics and dynamic changes

The contrast-enhanced CT (CECT) did not accurately reveal the inflammation level of irAP. It showed a normal contour of pancreas and homogeneous enhancement of pancreatic parenchyma in the patients with mild and moderate irAP (Figure 2(a) and 3(b)). Even in the patient with severe irAP, the morphological change was undetectable and the enhancement of the pancreatic parenchyma was homogeneous (Figure 1(c)).

Alternatively, MRI was a sensitive imaging method that could clarify the level of pancreatic inflammation from mild to severe. In the mild irAP patient, the T1-weighted fat-saturated (T1W FS) image showed slightly decreased signal intensity of the pancreas, which was lower compared to the liver (Figure 3(c)). DWI demonstrated markedly increased signal intensity of the pancreas, suggesting diffusion restriction (Figure 3(d)). In the patient with moderate irAP, the T1W FS had also slightly decreased and inhomogeneous signal intensity of pancreas (Figure 2(b)), and DWI showed slightly increased and inhomogeneous signal intensity of the pancreas (Figure 2(c)). In the patient with severe irAP, T1W FS showed a slightly enlarged pancreatic body and tail with decreased signal intensity, which was hypointense relative to the liver (Figure 1(a)). DWI showed markedly increased signal intensity of the pancreatic parenchyma, which was significantly higher compared to the spleen and the kidney (Figure 1(b)). Magnetic resonance cholangiopancreatography (MRCP) showed narrowing of the distal common bile duct (CBD) and main pancreatic duct (MPD) (Figure 1(f)). The imaging manifestations of severe irAP are different from traditional severe AP. There was no typical peripancreatic exudation, fluid collection, necrosis, etc. Instead, it was more akin to AIP.

In the patient with severe irAP, the two- and eight-week marks after glucocorticoid treatment can be considered as important monitoring timepoints in MRI. Two weeks after glucocorticoid treatment, the MRI already showed significant improvement, with a decrease in size of the pancreatic body and tail. The signal intensity recovery increased in T1W FS image, but remained lower than liver (Figure 1(d)). The signal intensity recovery decreased in DWI, suggesting less severe diffusion restriction (Figure 1(e)). Eight weeks later, the inflammation had recovered nearly to normal. The pancreatic body and tail further decreased in size and appeared atrophic. The signal intensity of the pancreas further increased to isointense to liver in the T1W FS image (Figure 1(g)). The high signal intensity of the pancreas further decreased in DWI, only slightly higher than the spleen suggesting residual inflammation (Figure 1(h)). MRCP showed resolution of the strictures of the distal CBD and MPD (Figure 1(i)). Finally, after 22 weeks of glucocorticoid treatment with normalized sAMY and sLIP, T1W FS image showed the pancreatic body and tail were atrophic, and the signal intensity of the pancreas was still isointense to liver (Figure 1(j)). DWI showed the signal intensity of the pancreas was still slightly higher than the spleen (Figure 1(k)). MRCP showed that the MPD stricture had resolved, but an irregular pattern remained (Figure 1(l)).

The utility of MRI findings of β-cell destruction was minor or negligible. After the recovery of moderate irAP and at the onset of severe pancreatic β-cell destruction, the CECT did not show any noticeable change (Figure 2(d)). T1W FS image showed slightly increased pancreatic signal intensity, which remained lower than normal (Figure 2(e)). DWI showed more homogeneous signal intensity of the pancreas, which remained higher than normal (Figure 2(f)).

Treatment and outcome

Traditional therapy includes fasting, intravenous hydration and proton pump inhibitors (PPI). Four of the six patients received traditional therapy, one of whom received a combination of traditional and glucocorticoid therapy, three other patients received the traditional therapy alone, and all patients had partial or complete relief of inflammation. Abdominal pain completely resolved in the patient with moderate irAP, and sAMY/sLIP normalized after traditional treatment alone. In the patient with severe irAP, the abdominal pain was completely relieved, and sAMY and sLIP decreased 46% and 29%, respectively after traditional treatment alone in seven days, with no further decrease after one further week (Table S1).

Glucocorticoids were the primary treatment in patients with moderate and severe irAP. The response was somewhat similar to AIP, with an early rapid initial effect followed subsequently by a slow recovery. In the patient with severe irAP, after two weeks of prednisone, the sAMY and sLIP decreased from 686 U/L to 498 U/L and 10 517 U/L to 5002 U/L, and the MRI showed significant improvement. Eight weeks later, the patient's sAMY and sLIP further dropped to 215 U/L and 1219 U/L, inflammation further recovered in MRI; however, imaging suggested that there was residual inflammation. Finally, as prednisone was tapered gradually to 10 mg for

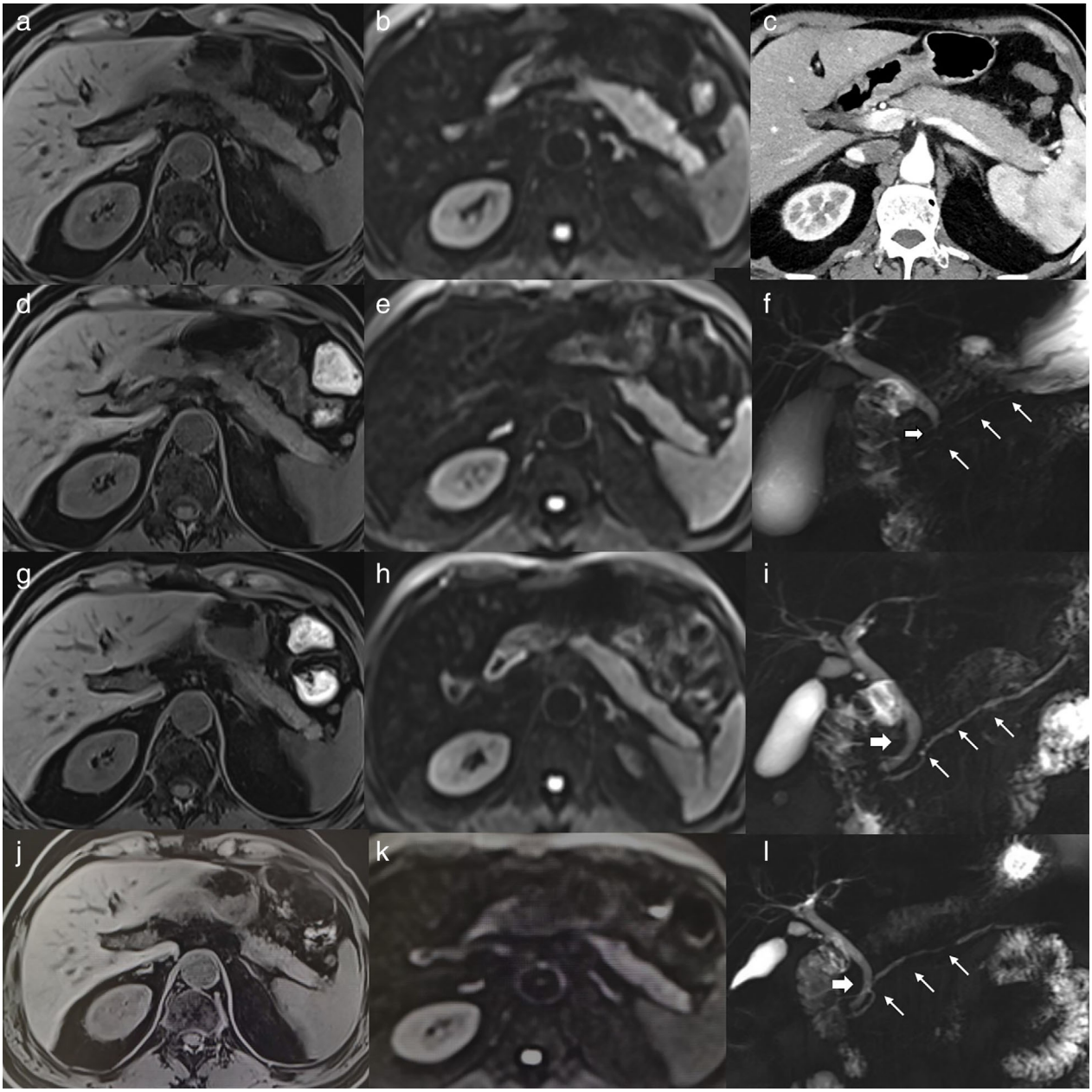

FIGURE 1 The radiological characteristics and dynamic changes of the patient with severe immune-related acute pancreatitis (irAP). (a) The T1-weighted fat-saturated (T1W FS) image at the onset of severe irAP. (b) The diffusion-weighted image (DWI) image at the onset of severe irAP. (c) The contrast-enhanced CT (CECT) image at the onset of severe irAP. (d) The T1w fs image after two weeks of glucocorticoid treatment. (e) The DWI image after two weeks of glucocorticoid treatment. (f) The magnetic resonance cholangiopancreatography (MRCP) showed narrowing of the distal common bile duct (CBD, thick arrow) and main pancreatic duct (MPD, thin arrows), at the onset of severe irAP. (g) The T1W FS image after eight weeks of glucocorticoid treatment. (h) The DWI image after eight weeks glucocorticoid treatment. (i) The MRCP image after eight weeks glucocorticoid treatment. (j) The T1W FS image after 22 weeks of glucocorticoid treatment. (k) The DWI image after 22 weeks of glucocorticoid treatment. (l) The MRCP image after 22 weeks of glucocorticoid treatment

maintenance, sAMY and sLIP gradually decreased to 112 U/L and 285 U/L within the normal range, and manifestation recovered almost to normal on MRI (Figure 1 and S1, Table S2).

Reinitiation of immune checkpoint inhibitors

According to the NCCN guideline for management of immune checkpoint inhibitor-related toxicities,[12] three of six patients resumed the ICIs, with deterioration, stable disease and development of other irAEs, respectively. The first Asy-sAMY/sLIP-Elv patient had aggravation to moderate irAP; the second Asy-sAMY/sLIP-Elv patient had stable sAMY/sLIP levels. The patient with moderate irAP experienced severe pancreatic β-cell destruction without irAP recurrence. This patient had CR to SCLC, and the anti-PD-1 treatment was restarted after complete recovery of irAP. He subsequently developed severe pancreatic β-cell destruction manifesting as type I diabetes mellitus (T1DM) with diabetic

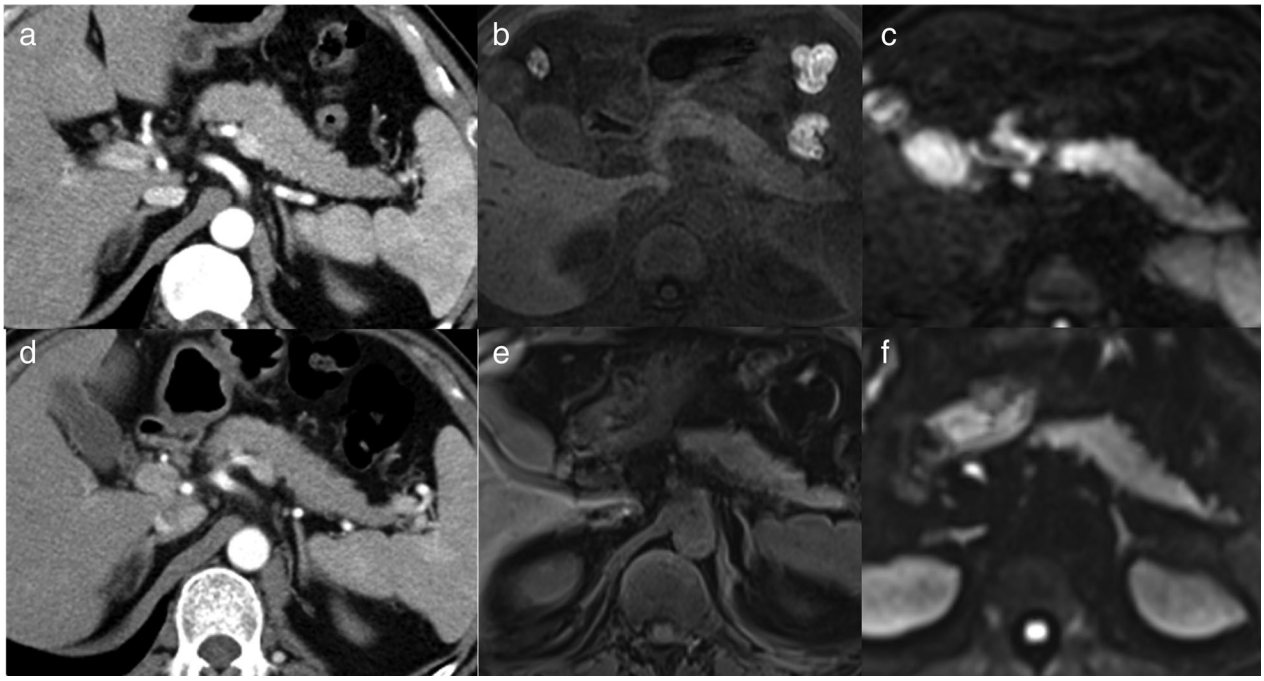

FIGURE 2 The radiological characteristics and dynamic changes of moderate immune-related acute pancreatitis (irAP) and pancreatic β-cell destruction. (a) The contrast-enhanced CT (CECT) image at the onset of moderate irAP. (b) The T1-weighted fat-saturated (T1W FS) image at the onset of moderate irAP. (c) The diffusion-weighted image (DWI) image at the onset of moderate irAP. (d) The CECT image at the onset of pancreatic β-cell destruction with irAP recovery. (e) The T1W FS image at the onset of pancreatic β-cell destruction with irAP recovery. (f) The DWI image at the onset of pancreatic β-cell destruction with irAP recovery

ketoacidosis (DKA), as well subclinical hyperthyroidism without irAP recurrence. After the DKA had been corrected and his glucose level was stabilized with insulin, he resumed anti-PD-1 therapy. Unfortunately, his subclinical hyperthyroidism deteriorated to thyrotoxicosis (Table S1).

Intestinal microbiota

Baseline microbiota of irAP patients

At the phylum level, the histogram showed that the relative abundance of *Firmicutes* was high and *Bacteroidetes* was low in Pt.1A and Pt.3A compared to Pt.2A (Figure 4(a), Table S7). At the genus level, the histogram showed the relative abundance of *Alistipes* and *Bacteroides* were low, while *Lachnospiraceae* was high in Pt.1A and Pt.3A compared to Pt.2A. (Figure 4(b), Table S7).

Dynamic change of microbiota pre- and post-treatment in irAP patients

According to the flower plot of OTUs and PCoA analysis by Bray-Curtis, the microbiota had dynamic self-change between pre- and post-treatment in the patient with severe irAP (Figure 4(c) and 4(g) and Figure S3A). The α diversity observed species, Shannon, Simpson, Chao1 and ACE index were higher in Pt. 1C, compared Pt. 1A, Pt. 1B, Pt. 1D and Pt. 1E (Table S8). The rank abundance curve also showed that Pt.1C had the highest richness and evenness (Figure 4(d)).

At the phylum level, the histogram showed the relative abundance of *Firmicutes* was high and *Bacteroidetes* was low in Pt. 1A compared to Pt.1B-1E (Figure 4(e) and Table S7). At the genus level, the histogram and line graph showed the relative abundance of *Alistipes* and *Bacteroides* were low, while *Blautia*，*Lachnospiraceae*, and *Faecalibacterium* were high in Pt. 1A compared to Pt.1B-1E (Figure 4(f) and Figure S3B, Table S7).

DISCUSSION

Pancreatic irAEs are a new challenge for gastroenterologists. The spectrum of irAP is quite heterogeneous, and manifestations vary from Asy-sAMY/sLIP-Elv to symptomatic irAP resulting in an emergency department visit.[14] The prevalence of pancreatic irAEs is increasing due to the wide use of ICIs; however, little is known about them. Thus, the awareness, recognition and management of this clinical entity is imperative.[15]

First, due to the common combination therapies of chemotherapy and immunotherapy, the differential diagnosis of ICI-related pancreatitis and chemotherapy drug-related pancreatitis is key and challenging. In our case series, three patients had pancreatic irAEs during anti-PD-1 monotherapy. Three other patients received chemotherapy

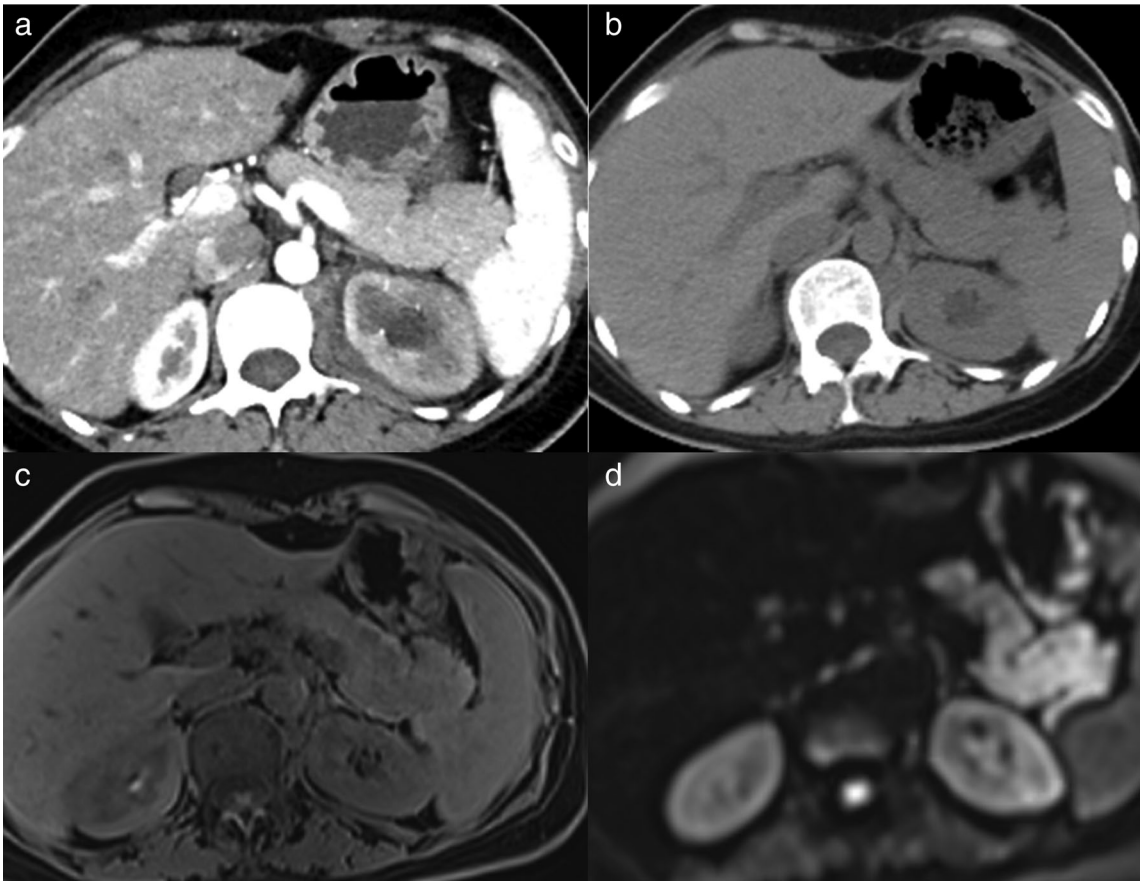

FIGURE 3 The radiological characteristics and dynamic changes of mild immune-related acute pancreatitis (irAP). (a) The contrast-enhanced computed tomography (CECT) image at baseline of tumor assessment before immune checkpoint inhibitors (ICI) treatment. (b) The noncontrast computed tomography (CT) at the onset of mild irAP. (c) The T1-weighted fat-saturated (T1W FS) at the onset of mild irAP. (d) The diffusion-weighted image (DWI) at the onset of mild irAP

including etoposide, carboplatin, paclitaxel and pemetrexed, combined with anti-PD-1 therapy when pancreatic irAE occurred. Among all these chemotherapy drugs, only paclitaxel has been listed as class III according to the drug-induced acute pancreatitis classification system, which means that there are only 2–4 cases reported in the literature without consistent latency.[16] However, after recovery from mild pancreatic irAE, the patient in this study resumed chemotherapy with paclitaxel and carboplatin without pancreatitic relapse. Thus, all these six patients could be excluded from chemotherapy drug-related pancreatitis.

Further, we identified the following clinical characteristics of pancreatic irAEs. First, pancreatic irAEs could occur in patients of different gender, age and tumor. Second, pancreatic irAEs occurred after single or multiple cycles of ICIs monotherapy or combined therapy. The duration from first or last ICIs to irAEs onset was variable with a median of 105 and 5.5 days. Third, all patients had an effective response to immunotherapy with SD, PR and CR. Ishihara et al. found that irAE development was an independent prognostic factor of progression-free survival (PFS) in a multivariate analysis (hazard ratio 0.25, $p = 0.0009$), and the median PFS was significantly longer in patients with irAEs than in those without irAEs (13.1 vs. 4.87 months, $p < 0.0001$).[3] Considering that ICIs activate T cell immunity, irAEs are bound to occur with good antitumor effects. Fourth, abdominal pain corresponded to the severity of pancreatic irAEs, and the mild to severe irAP patients manifested nonexistent to severe abdominal pain. Abu-Sbeih et al. concluded that irAP patients with clinical symptoms were associated with more pronounced sLIP increase, imaging pancreatitis, intravenous fluids, and steroid treatment.[3] Finally, pancreatic irAEs could be accompanied by other mild to severe irAEs, for example, a dermatological AE, colitis or hepatoxicity.

In our case series, the characteristics of laboratory results were as follows. First, sAMY and sLIP were paralleled to clinical conditions, and ideal markers to assess and monitor pancreatic irAE severity. Patients with severe irAP had both sAMY and sLIP far greater than a three-fold increase, and patients with mild irAP may have single three-fold increase of sAMY or sLIP. Second, serum IgG4 could increase in patients with severe irAP, did not fulfill the criterion of IgG4-related disease. Third, theoretically, T lymphocyte subsets may reflect the activation of $CD8^+$ T cells by ICIs. However, among peripheral blood T lymphocyte subsets, only

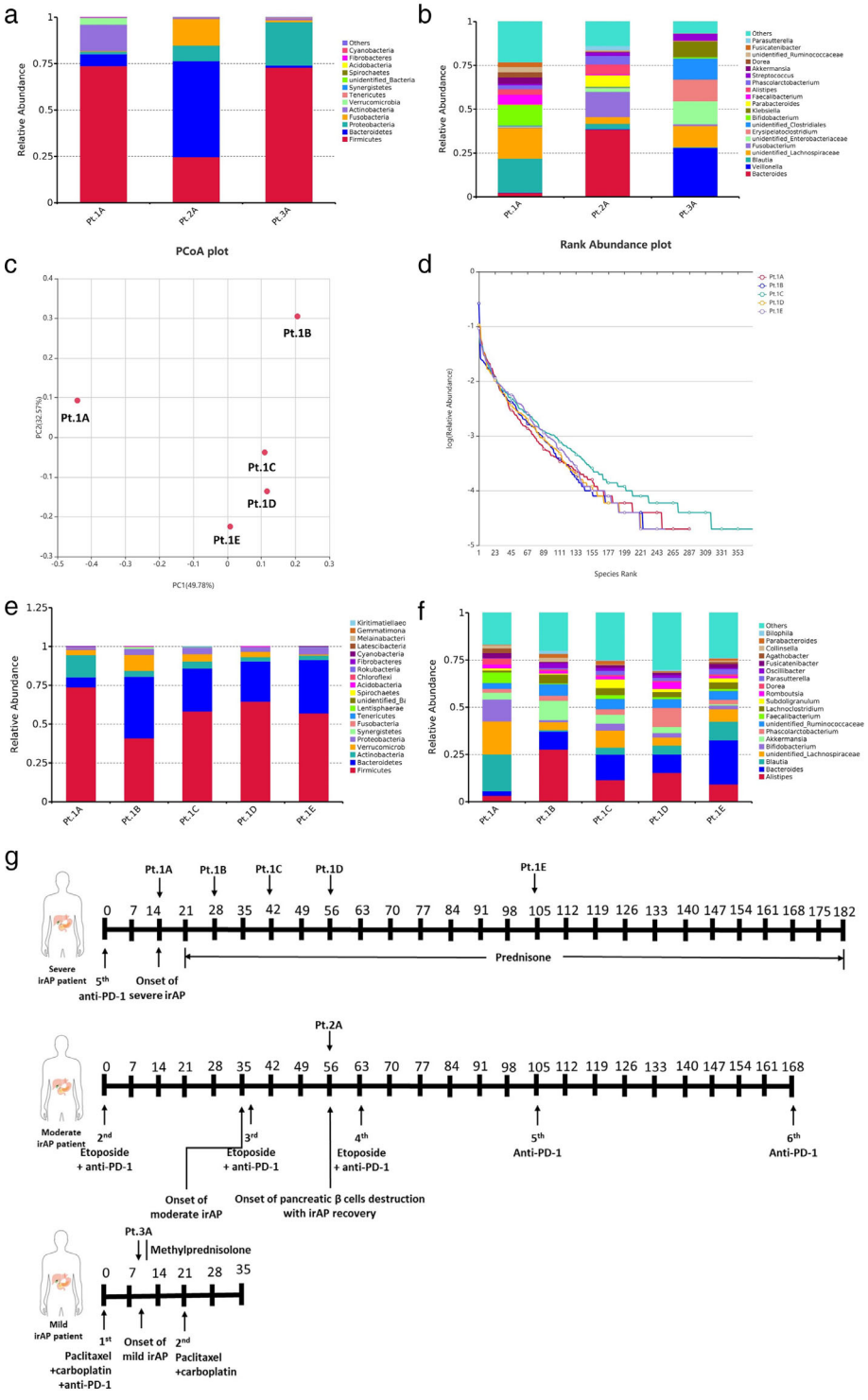

FIGURE 4 The dynamic changes of microbiota at baseline and post-treatment in three immune-related acute pancreatitis (irAP) patients. (a) Histogram of baseline microbiota of three cases at phylum levels. (b) Histogram of baseline microbiota of three cases at genus levels; (c) PCoA analysis by Bray-Curtis in a patient with severe irAP. (d) Rank abundance curve of a patient with severe irAP. (e) Histogram of microbiota of a patient with severe irAP at phylum levels. (f) Histogram of microbiota of severe irAP patient at genus levels. (g) Time points of fecal sampling and various treatments in three irAP patients. Pt.1A: Onset of irAP in a patient with severe irAP; Pt.1B: two weeks after glucocorticoid treatment in a patient with severe irAP; Pt.1C: four weeks after glucocorticoid treatment in a patient with severe irAP; Pt. 1D: six weeks after glucocorticoid treatment in a patient with severe irAP; Pt. 1E: 13 weeks after glucocorticoid treatment in a patient with severe irAP. Pt. 2A: Onset of pancreatic β-cell destruction with irAP recovery in a patient with moderate irAP. Pt. 3A: Onset of irAP in a patient with mild irAP

the percentage of HLA-DR$^+$CD8$^+$ in CD8$^+$ T cell had non-parallel increased in all six patients. Considering the tissue T lymphocyte subsets maybe a more ideal alternative choice.[17]

In our case series, the characteristics of radiological characteristics were as follows. First, CECT did not effectively assess the inflammation of irAP. It was commonly normal in patients with mild to moderate irAP and near normal in severe irAP. Among the limited irAP studies, Abu-Sbeih et al. reported only 17% irAP patients had pancreatitic findings, mainly pancreatic enlargement and heterogeneity on CT.[3] Second, MRI is a sensitive and ideal imaging method. MRI/MRCP is considered to be the safest, sensitive and effective imaging technique for the evaluation of pancreas and ductal system.[18] It can effectively differentiate irAP from traditional AP or CP.[15] The dynamic changes in MRI can also be used for monitoring during treatment. Third, the imaging manifestations of severe irAP could be similar to AIP. Finally, the MRI findings of irAP are more

obvious due to the main attacks of pancreatic acini and ducts. However, the MRI findings of severe β-cell destruction are minor or negligible.

In our case series, the characteristics of treatment and outcome were as follows. First, the traditional treatments including fasting, intravenous hydration, and PPIs could partially relieve inflammation. Intravenous fluid plays an important role in irAP treatment and even decreases the risk of long-term adverse outcomes.[3] Hence, intravenous fluid administration was encouraged, even in asymptomatic patients within 48 h of onset.[3] Second, in patients with moderate to severe irAP, glucocorticoids were the main treatment with rapid-slow effect. Hence, a high enough initial dosage and very slow tapering of glucocorticoids may be important.[19,20] Finally, after restarting treatment of ICIs, the patient may have deterioration, stable disease, or develop other kinds of irAE without irAP recurrence. Anti-PD-1 therapy occasionally caused fulminant diabetes with complete destruction of pancreatic β-cells resulting in DKA. This process is different from traditional T1DM, as anti-islet cell antibody (ICA), anti-glutamate decarboxylase antibody (GAD), and anti-insulin antibody (IAA) were all negative.[21] Acute autoimmune insulin-dependent diabetes presented with insulinopenia with undetectable C-peptide, which was caused by the acute and severe β-cell destruction after sudden and major activation of β-cell-reactive CD8+ T-cell clones.[22] The possible involvement of pancreatitis in this fulminant diabetes is still under debate; indeed, 42% of patients had evidence of pancreatitis at the time of onset of DM in a previous case series.[23] The rescue therapy of glucocorticoids after onset of ICI-induced DM would be ineffectual, and insulin therapy is needed and discontinuation of ICIs is not required.[22]

To our knowledge, there has been no previous study of the microbiota in irAP patients. Interestingly, animal experiments showed that AIP significantly deteriorated after cohousing or FMT from mice with severe AIP to mice with mild AIP, suggesting that the microbiota mediates experimental AIP.[24] In our case series, the microbiota of irAP patients had dynamic changes between baseline and post-treatment. The α diversity was low at baseline, and richness and evenness recovered best four weeks after glucocorticoid treatment. The baseline microbiota of irAP had a low *Bacteroidetes*/*Firmicutes* ratio at the phylum level compared to the case with pancreatic β-cell destruction. Previous studies showed the patients with low *Bacteroidetes*/*Firmicutes* ratios were prone to better clinical responses and ICI-related colitis.[8,25] In pancreatic disease, the AIP patients had lower *Bacteroides* species than CP patients.[12] However, the taxonomic changes of microbiota associated with T1DM are relatively modest.[26] All these were consistent with our microbiota results. The baseline microbiota of irAP had low relative abundance of *Alistipes* and *Bacteroides* with high *Lachnospiraceae* at the genus level, compared to the case of pancreatic β-cell destruction. The *Bacteroidetes*/*Firmicutes* balance might be a potential intervention target, and may prevent the occurrence and recurrence of irAP, but further study is warranted.

In conclusion, the pancreatic irAEs could occur after single or multiple cycles of ICI therapy. The patients were prone to have an effective response to immunotherapy. The abdominal pain was mainly clinical manifestation, and sAMY/sLIP changes were parallel with disease severity. Instead of contrast-enhanced CT, MRI is a sensitive and ideal imaging modality for assessment and monitoring. The imaging of severe irAP could be more akin to AIP with IgG4 mild increase. The traditional treatment could partially relieve the inflammation. Glucocorticoids were the main treatment with rapid-slow effect. After resuming ICI therapy, the pancreatic irAE could deteriorate, remain stable or develop other irAEs (e.g., severe pancreatic β-cell destruction) without irAP recurrence. Interestingly, the microbiota had relative changes in the balance between *Bacteroidetes*/*Firmicutes* at baseline and during treatment.

The main limitation of our case series was the small number of patients. Taking into account the rarity of irAP, large-scale clinical studies are relatively difficult to achieve. Hence, we put our best effort to provide and conclude the characteristics of clinical-imaging manifestations, laboratory results, and microbiota changes. We anticipate and believe that these provide useful insight to the recognition, management, and potential prevention of recurrent pancreatic irAEs. We hope this information allows more patients with malignant disease to experience improved survival outcomes through uninterrupted immunotherapy.

ACKNOWLEDGMENTS

This study was supported by the General Program of Natural Science Foundation of Beijing Municipality [No.7192172], the Youth Program of National Natural Science Foundation of China [No.82000526; No. 82003309]. We would like to express our sincere gratitude to Dr. Ritchell van Dams, MD, MHS from Department of Radiation Oncology, University of California, Los Angeles, for his review and extensive editing of the manuscript.

CONFLICT OF INTEREST

All authors declare no conflict of interests.

ORCID

Bei Tan https://orcid.org/0000-0002-0053-7399
Min-jiang Chen https://orcid.org/0000-0002-4040-6115
Yan Xu https://orcid.org/0000-0002-2832-2664

REFERENCES

1. George J, Bajaj D, Sankaramangalam K, Yoo JW, Joshi NS, Gettinger S, et al. Incidence of pancreatitis with the use of immune checkpoint inhibitors (ICI) in advanced cancers: a systematic review and meta-analysis. Pancreatology. 2019;19:587–94.
2. El Majzoub I, Qdaisat A, Thein KZ, Win MA, Han MM, Jacobson K, et al. Adverse effects of immune checkpoint therapy in cancer patients visiting the emergency department of a comprehensive cancer center. Ann Emerg Med. 2019;73:79–87.
3. Abu-Sbeih H, Tang TL, Lu Y, Thirumurthi S, Altan M, Jazaeri AA, et al. Clinical characteristics and outcomes of immune checkpoint inhibitor-induced pancreatic injury. J Immunother Cancer. 2019;7:31.

4. Routy B, Le Chatelier E, Derosa L, Duong CPM, Alou MT, Daillère R, et al. Gut microbiome influences efficacy of PD-1-based immunotherapy against epithelial tumors. Science. 2018;359:91–7.
5. Gopalakrishnan V, Spencer CN, Nezi L, Reuben A, Andrews MC, Karpinets TV, et al. Gut microbiome modulates response to anti-PD-1 immunotherapy in melanoma patients. Science. 2018;359:97–103.
6. Matson V, Fessier J, Bao R, Chongsuwat T, Zha Y, Alegre M-L, et al. The commensal microbiome is associated with anti-PD-1 efficacy in metastatic melanoma patients. Science. 2018;359:104–8.
7. Vétizou M, Pitt JM, Daillère R, Lepage P, Waldschmitt N, Flament C, et al. Anticancer immunotherapy by CTLA-4 blockade relies on the gut microbiota. Science. 2015;350:1079–84.
8. Chaput N, Lepage P, Coutzac C, Soularue E, le Roux K, Monot C, et al. Baseline gut microbiota predicts clinical response and colitis in metastatic melanoma patients treated with ipilimumab. Ann Oncol. 2017;28:1368–79.
9. Wang Y, Wiesnoski DH, Helmink BA, Gopalakrishnan V, Choi K, DuPont HL, et al. Fecal microbiota transplantation for refractory immune checkpoint inhibitor-associated colitis. Nat Med. 2018;24(12):1804–8.
10. Wang F, Yin Q, Chen L, Davis MM. Bifidobacterium can mitigate intestinal immunopathology in the context of CTLA-4 blockade. Proc Natl Acad Sci U S A. 2018;115:157–61.
11. Wang T, Zheng N, Luo Q, Jiang L, He B, Yuan X, et al. Probiotics *Lactobacillus reuteri* abrogates immune checkpoint blockade associated colitis by inhibiting group 3 innate lymphoid cells. Front Immunol. 2019;10:1235.
12. Hamada S, Masamune A, Nabeshima T, Shimosegawa T. Differences in gut microbiota profiles between autoimmune pancreatitis and chronic pancreatitis. Tohoku J Exp Med. 2018;244:113–7.
13. Thompson JA, Schneider BJ, Brahmer J, Andrews S, Armand P, Bhatia S, et al. NCCN guidelines insights: management of immunotherapy-related toxicities, version 1.2020. J Natl Compr Canc Netw. 2020;18:230–41.
14. Michot JM, Ragou P, Carbonnel F, Champiat S, Voisin AL, Mateus C, et al. Significance of immune-related lipase increase induced by antiprogrammed death-1 or death ligand-1 antibodies: a brief communication. J Immunother. 2018;41:84–5.
15. Porcu M, Solinas C, Migali C, Battaglia A, Schena M, Mannelli L, et al. Immune checkpoint inhibitor-induced pancreatic injury: imaging findings and literature review. Target Oncol. 2020;15:25–35.
16. Badalov N, Baradarian R, Kadirawel I, Li J, Steinberg W, Tenner S, et al. Drug-induced acute pancreatitis: an evidence-based review. Clin Gastroenterol Hepatol. 2007;5:648–61.
17. Yoneda S, Imagawa A, Hosokawa Y, Baden MY, Kimura T, Uno S, et al. T-lymphocyte infiltration to islets in the pancreas of a patient who developed type 1 diabetes after administration of immune checkpoint inhibitors. Diabetes Care. 2019;42:e116–8.
18. Drake LM, Anis M, Lawrence C. Accuracy of magnetic resonance cholangiopancreatography in identifying pancreatic duct disruption. J Clin Gastroenterol. 2012;46:696–9.
19. Hsu C, Marshall JL, He AR. Workup and management of immune-mediated hepatobiliary pancreatic toxicities that develop during immune checkpoint inhibitor treatment. Oncologist. 2020;25:105–11.
20. Kohlmann J, Wagenknecht D, Simon JC, Ziemer M. Immune-related pancreatitis associated with checkpoint blockade in melanoma. Melanoma Res. 2019;29:549–52.
21. Yilmaz M. Nivolumab-induced type 1 diabetes mellitus as an immune-related adverse event. J Oncol Pharm Pract. 2020;26:236–9.
22. Marchand L, Disse E, Dalle S, Reffet S, Vouillarmet J, Fabien N, et al. The multifaceted nature of diabetes mellitus induced by checkpoint inhibitors. Acta Diabetol. 2019;56:1239–45.
23. Stamatouli AM, Quandt Z, Perdigoto AL, Clark PL, Kluger H, Weiss SA, et al. Collateral damage: insulin-dependent diabetes induced with checkpoint inhibitors. Diabetes. 2018;67:1471–80.
24. Kamata K, Watanabe T, Minaga K, Hara A, Yoshikawa T, Okamoto A, et al. Intestinal dysbiosis mediates experimental autoimmune pancreatitis via activation of plasmacytoid dendritic cells. Int Immunol. 2019;31:795–809.
25. Dubin K, Callahan MK, Ren B, Khanin R, Viale A, Ling L, et al. Intestinal microbiome analyses identify melanoma patients at risk for checkpoint blockade-induced colitis. Nat Commun. 2016;7:1039.
26. Gavin PG, Hamilton-Williams EE. The gut microbiota in type 1 diabetes: friend or foe? Curr Opin Endocrinol Diabetes Obes. 2019;26:207–12.

SUPPORTING INFORMATION

Additional supporting information may be found online in the Supporting Information section at the end of this article.

How to cite this article: Tan B, Chen M-j, Guo Q, et al. Clinical-radiological characteristics and intestinal microbiota in patients with pancreatic immune-related adverse events. *Thorac Cancer*. 2021; 12:1814–1823. https://doi.org/10.1111/1759-7714.13990